THE STRUCTURAL STRESS METHOD FOR THE FATIGUE ANALYSIS OF WELDED STRUCTURES

Authors: Pingsha Dong, John Draper

Center for Welded Structures Research, **BATTELLE**, Columbus, OH, **dongp@battelle.org**

Safe Technology Limited, Sheffield, UK, john.draper@safetechnology.com

The stress concentration in a welded joint dominates the fatigue behaviour of the joint. However, traditional finite element methods are not capable of consistently capturing the stress concentration effects due to their mesh-sensitivity. A robust stress analysis procedure has recently been developed at Battelle and extensively validated by various industries. The method is called Verity® mesh-insensitive structural stress method and serves as a FE post-processing procedure to commercial FE packages. The Verity® method has been integrated into fe-safe™ and is available from Safe Technology Limited. The method is based on the mapping of the balanced nodal forces/moments along an arbitrary weld line into the work-equivalent tractions (or line forces/moments). A complex stress state due to notch effects can then be represented in the form of a simple stress state in structural mechanics in terms of through-thickness membrane and bending components at each nodal location. The resulting structural stress calculations are mesh-insensitive as long as the overall geometry of a component is reasonably represented in a finite element model. In addition to its mesh-insensitivity, the effectiveness of the structural stress parameter has been further validated by collapsing several thousands of fatigue tests available from literature into a single fatigue life curve, referred to as the master S-N curve.

1 INTRODUCTION

Fatigue design and evaluation of welded joints are typically carried out by a weld classification approach in which a family of parallel nominal stress based S-N curves are used according to joint types and loading modes [1]. In all the global based stress analysis procedures (such as nominal stress, extrapolation based hot spot stresses, etc.) for fatigue evaluation purposes [1-6], the ultimate goal is to identify an appropriate stress parameter which can be consistently calculated in practice, and can be used to effectively correlate S-N data from various joint types and loading modes. This can be restated as both the necessary and sufficient conditions for seeking a global stress-based fatigue correlation parameter as follows:

(a) A global stress parameter must be able to be calculated consistently with a minimum mesh-sensitivity (mesh sizes, element shapes, element types, etc.) at a fatigue prone location such as at weld toe;

(b) Such a stress parameter must be demonstrated to be capable of correlating different fatigue behaviours (such as S-N data) observed in various joint types, loading modes, etc.

Obviously, nominal stress definition, if applicable for some joint configurations, satisfies the necessary conditions (a), since it can be calculated by simple formulae, i.e., without mesh-sensitivity. However, it is well known that the nominal stress definition does not satisfy the sufficient conditions (b), since it cannot be used to correlate S-N data from various joint types and loading modes. This is why a family of essentially parallel S-N curves has been used with respect to the nominal stress parameter as shown in Fig. 3 [1].

The fact that those S-N curves (Fig. 3) are essentially parallel to one another suggests the existence of a master S-N curve. A scaling parameter that correctly measures the stress concentration in various welded joint types and loading modes should be able to collapse all the parallel S-N curves in Fig. 3 into a single master S-N curve. It is the purpose of this paper to present such an approach by formulating an effective global stress parameter which can be used as a basis to establish such a master S-N curve. In this context, the nodal force (always implying moments in this paper) based mesh-insensitive structural stress method (5-9) will be briefly highlighted for its consistency in stress concentration characterization as required by the necessary conditions stated above. Then, the nodal force based (referred to as structural stress method throughout this paper) structural stresses are shown to possess a unique property which can be used for a rapid estimation of the stress intensity factors (K) in an arbitrary joint within a fracture mechanics context. As a result, a two-stage crack growth model has been proposed and validated by a large amount of experimental data. The two-stage growth law unifies both the conventional "short crack" anomalous crack growth and long cracks. By integrating the two-stage crack growth model, a unique scaling parameter encompassing the structural stress based stress concentration effects, loading mode effects, and thickness effects is then formulated and validated by a massive amount of historical weld fatigue S-N data from 1947 to present.

2 THE STRUCTURAL STRESS METHOD

The essence of the new structural stress method was based on the following considerations for fatigue evaluations of welded joints:

(a) It was postulated that the stress concentration at a fatigue prone location, such as a weld toe as shown in Fig. 4a, can be represented by an equilibrium-equivalent simple stress state (as shown in Fig. 4b) and self-equilibrium stress state (as shown in Fig. 1c). The former describes a stress state corresponding to an equivalent far field stress state in fracture mechanics context [4,6], or simply, a generalized nominal stress state at the same location, while the latter can be estimated by introducing a characteristic depth t_I as shown in Fig. 1 (dashed lines), as discussed in detail in [8];

(b) Within the context of displacement-based finite element methods, the balanced nodal forces and moments within each element automatically satisfy the equilibrium conditions at every nodal position. Therefore, the equilibrium-equivalent structural stress state in the form of membrane and bending stresses can be calculated by using the nodal forces/moments at a location of concern.

2.1 Shell/Plate Element Procedures

In order to calculate the structural stresses in terms of membrane and bending components, line forces and moments must be properly formulated by introducing work-equivalent arguments as discussed in [8-9]. As an example of such formulation for a closed weld line (i.e., two ends of an arbitrarily curve weld overlap each other, such as in a tubular joint), the nodal forces can be related to line forces along an arbitrarily curved weld as:

$$\begin{Bmatrix} F_1 \\ F_2 \\ F_3 \\ . \\ . \\ F_{n-1} \end{Bmatrix} = \begin{bmatrix} \frac{(l_1+l_{n-1})}{3} & \frac{l_1}{6} & 0 & \frac{l_{n-1}}{6} \\ \frac{l_1}{6} & \frac{(l_1+l_2)}{3} & \frac{l_2}{6} & 0 \\ 0 & \frac{l_2}{6} & \frac{(l_2+l_3)}{3} & \frac{l_3}{6} \\ 0 & 0 & \cdots & \cdots \\ \frac{l_{n-1}}{6} & 0 & \frac{l_{n-2}}{6} & \frac{(l_{n-2}+l_{n-1})}{3} \end{bmatrix} \begin{Bmatrix} f_1 \\ f_2 \\ f_3 \\ . \\ . \\ f_{n-1} \end{Bmatrix} \quad (1)$$

In the above equation, a closed weld line is assumed (the first node at the weld start is the same node at the weld end, such as a tubular joint), i.e., $F_n = F_1$ and $f_n = f_1$. The lowercase $f_1, f_2, ..., f_{n-1}$ are line forces along y'. In the matrix on the left hand of Eq. (1), l_i (i =1, 2, …, n-1) represents the element edge length projected onto the weld toe line from i^{th} element. The corresponding line moments can be calculated in an identical manner by replacing balanced nodal forces $F_1, F_2, ..., F_{n-1}$ in local y' direction with balanced nodal moments $M_1, M_2, ..., M_{n-1}$ with respect to x' in Eq. (1) above, as depicted in Fig. 5. Note that nodal force F_i in Eq. (1) represent the summation of the nodal forces at node i from the adjoining weld toe elements situated on the positive side of y' axis, as shown in Fig. 5. Before Eq. (1) can be constructed, coordinate transformation for the nodal forces and nodal moments from the global x-y-z to local x'-y'-z' axis system must be performed, with x' traveling along the weld line and y' being perpendicular to the weld line. All these calculations have been automated as a structural stress post-processor. The linear system of equations described by Eq. (1) can be solved simultaneously to obtain line forces for all nodes along the line connecting all weld toe nodes. Substituting the corresponding nodal moments into Eq. (1), one obtains line moments in the same manner. Then, the structural stress shown in Fig. 4b at each node along the weld (such as the weld toe) can be calculated as:

$$\sigma_s = \sigma_m + \sigma_b = \frac{f_{y'}}{t} + \frac{6m_{x'}}{t^2} \qquad (2)$$

For parabolic plate or shell elements, Eq. (1) can be formulated in an identical fashion with the relationships provided in [8]. In-plane shear can be treated in an identical manner [8].

2.2 Calculation Examples

A tubular T-joint according to a recent round robin study on fracture assessment [5,9,10] is shown in Fig. 4a, where a detailed strain gauge measurements were also collected for deriving hot spot stress based stress concentration at the saddle positions as shown. To demonstrate the effectiveness of the present structural stress procedures, four shell element models with drastically different element sizes near the tube-to-tube weld are shown in Fig. 4a, varying approximately from 0.25tx0.25t, 0.5tx0.5t, 1tx1t, to 2tx2t. Note that the weld was not modeled at the tube-to-tube intersection in order to simplify the mesh generation efforts in the present mesh-sensitivity study.

Fig. 4b summarizes the structural stresses along the weld toe on the chord side obtained from the four shell models shown in Fig. 4a. Since the structural stresses along the weld possess the quarter symmetry, Fig. 4b shows only the results for a quarter of the weld length measured from the saddle point shown in Fig. 4a. The maximum structural stress concentration occurs at the saddle position. Within the angular span of 90^o along the 3D curved weld from saddle to crown positions, the 2tx2t mesh represents the weld line with only three nodal positions (or about two and half linear elements) as shown by the triangle symbols in Fig. 4b. Therefore, the difference in the structural stress calculations from the 2tx2t mesh is mainly due to the geometric changes at the weld line (tube to tube intersection) resulting from the large linear element sizes used. However, the structural stress based SCF at the saddle position is still within about 5% of the fine mesh case (.25tx.25t). Excluding the 2tx2t mesh, the SCF variations in the other three models are all within the 2% of each other.

As another example, the plate to I-beam joint, from Fricke [1], is analyzed here using the new structural stress procedures discussed above. In the models shown in Fig. 5a, the box fillet weld was modeled as simple nodal connections between attachment plate edge and I beam. The weld line in this instance is considered as being open-ended. The virtual node method as discussed in [9] is automatically activated in constructing Eq. (1). Four drastically different element sizes ranging from 0.5tx0.5t to 4tx4t are used in the mesh designs, as shown in Fig. 5a. The structural stress distributions (normalized by the nominal bending stress) calculated along the weld toe on the attachment plate side are shown in Fig. 5b. It can be seen that the variation in the structural stress calculated at the weld end positions is within about 1% for all four cases. The validity of the SCF was demonstrated using models with the fillet weld being properly represented by a row of inclined shell elements [9]. Note that in all four models shown in Fig. 5a, the weld is not modeled for simplicity. As the element sizes change at the beam-to-attachment intersection, the geometric representation remains the same even if a 4tx4t mesh is used. This is not the case for the tubular T-joint shown in Fig. 4 discussed earlier.

3 MASTER S-N CURVE FORMULATION

In seeking a stress-based scaling parameter to correlate the multiple S-N curves as shown in Fig. 1, it may be assumed that fracture mechanics principles are applicable, implying that crack propagation dominates fatigue lives in welded joints. The validity of such an assumption must be demonstrated by correlating a large amount of S-N test data.

3.1 Structural Stress Based K Estimation

Naturally, the simple candidate fracture mechanics parameter which can be considered for the current purpose is the stress intensity factor K. However, generalized K solutions are not available for welded joints. Fortunately, the structural stress definition (Fig. 2b) is consistent with the far-field stress definition (σ^{∞}) in fracture mechanics. Therefore, the structural stress calculation process can be viewed as a stress transformation process from an actual complex joint in a structure under arbitrary loading to a simple fracture specimen, in which the complex loading and geometry effects are captured in the form of membrane and bending, as shown in Fig. 6. As a result, K for any crack size along the weld can be estimated by using the existing K solution for a simple plate fracture mechanics specimen subjected to both membrane tension and bending, by considering either an edge crack or a surface elliptical crack.

The detailed derivations and validations can be found in [8]. For demonstration purposes, Fig. 7 shows the validation for considering an edge crack in a T fillet weld. In Fig. 7, the case corresponding to "W/O notch stress" was obtained by directly plugging the structural stress components (membrane and bending) calculated using the present structural stress method into the existing K solution for an edge notch specimen under remote tension and bending, respectively. The case "W/ notch stress" refers to the use of the self-equilibrating part of the stress state as well (Fig. 2c) which is analytically estimated, as discussed in [8].

It can be seen that without considering the notch stress (or self-equilibrating part of the stress state, Fig 2c) the current solution provides an accurate K estimation for crack size *a/t* larger than about 0.1. With the use of the notch stress effects, K can be calculated for any given infinitesimally small *a/t*. The current solution in Fig. 7 is higher for small *a/t* than the weight function solution from Glinka (see [8] for detail). This is because Glinka introduced a small weld toe radius in performing the finite element stress calculation to avoid the mesh-sensitivity. In the present calculations the weld toe radius was assumed to be zero, simulating a sharp notch at the weld toe.

3.2 A Two-Stage Growth Model

The non-monotonic K behaviour as a function of a/t shown in Fig. 7 is characteristic among all joint types investigated [8]. As the crack size *a/t* becomes smaller than *a/t* ~ 0.1 the elevated K is attributed to the dominance of the notch stresses at weld toe. It can then be postulated that both the short crack and long crack growth processes may be characterized by the two distinct stages of the K behaviour as a crack propagates from *a/t* < 0.1 to *a/t* > 0.1. Along this line, it can be argued that two stages of stress intensity solutions in the form of the notch-stress dominated $\Delta K_{a/t<0.1}$ and far-field stress dominated $\Delta K_{a/t>0.1}$ can be separated to characterize the full range crack growth behaviour from 0 <*a/t* <0.1 ("small crack") to $0.1 \leq a/t \leq 1$ ("long crack"). Here, the term ΔK refers to the stress intensity factor range corresponding to remote stress range. It then follows that:

$$\frac{da}{dN} = C\left[f_1(\Delta K)_{a/t\leq 0.1} \times f_2(\Delta K)_{a/t>0.1}\right] \qquad (3)$$

By introducing a stress intensity magnification factor M_{kn} in dimensionless form and assuming a power-law form of the two stage crack growths corresponding to $f_1(\Delta K)_{a/t\leq 0.1}$ and $f_2(\Delta K)_{a/t>0.1}$, respectively, Eq. (3) can be re-written as:

$$\frac{da}{dN} = C(M_{kn})^n (\Delta K_n)^m \qquad (4)$$

The terms M_{kn} and K_n are defined below:

$$M_{kn} = \frac{K(\text{with local notch effects})}{K_n(\text{based on through thickness } \sigma^t{}_{\mathrm{m}} \text{ and } \sigma^t{}_{\mathrm{b}})} \qquad (5)$$

signifying the notch-induced magnification of the stress intensity factors as *a/t* approaches zero. The constants *n* represents the crack growth exponent for the first stage of the crack growth and *m* the conventional Paris law exponent, both of which are to be determined by experimental crack growth rate data.

The validation of the two-stage growth model is shown in Fig. 8. The crack growth data were taken from well-known short crack growth data by Tanaka and Nakai [11] and Shin and Smith [12]. Without relying on any crack closure arguments, all the so-called anomalous crack growth data in Fig. 8a are collapsed into single straight data band in Fig. 8b, with a unified slope of m=3.6. Note that the first exponent in Eq. (4) was empirically determined as n=2. More detailed discussions on the notch stress formulation and the two stage growth law can be found in [13].

3.3 Equivalent Structural Stress Parameter

The two-stage crack (Eq. 4) with two stage growth exponents being $n = 2$ and $m = 3.6$, can be integrated as

$$N = \int_{a \to 0}^{a = a_f} \frac{da}{C\ (M_{kn})^n (\Delta K)^m} \qquad (6)$$

As discussed in [8,13], an extensive investigation of M_{kn} for various joint types showed that it can be approximated by a single curve as a function of *a/t* for all joint types once the denominator in Eq. (5) is formulated using the mesh-insensitive structural stress.

Note that the integral in Eq. (6) is not very sensitive to the final crack size a_f and therefore can be written in a relative crack length form as:

$$N = \int_{a_i/t \to 0}^{a/t = 1} \frac{t d(a/t)}{C(M_{kn})^n (\Delta K)^m} = \frac{1}{C} \cdot t^{1-\frac{m}{2}} \cdot (\Delta \sigma_s)^{-m} I(r) \qquad (7)$$

where $I(r)$ is a dimensionless function of bending ratio r ($r = \Delta\sigma_b / \Delta\sigma_s$) after performing the following integration for a given m:

$$I(r) = \int_{a_i/t \to 0}^{a/t = 1} \frac{d(a/t)}{(M_{kn})^n \left[f_m(\frac{a}{t}) - r\left(f_m(\frac{a}{t}) - f_b(\frac{a}{t}) \right) \right]^m}$$

Then, Eq. (7) can be expressed in terms of N once the dimensionless I(r) function is known:

$$\Delta\sigma_s = C^{-\frac{1}{m}} \cdot t^{\frac{2-m}{2m}} \cdot I(r)^{\frac{1}{m}} \cdot N^{-\frac{1}{m}} \qquad (8)$$

Eq. (8) uniquely describes a family of an infinite number of structural stress based *S-N* curves ($\Delta\sigma_s - N$) as a function of thickness effects (t), and bending ratio effects r. If Eq. (8) provides a good representation of the fatigue behaviour of welded joints, an equivalent structural stress parameter can be defined

by normalizing the structural stress range $\Delta\sigma_s$ with the two variables expressed in terms of t and r on the right hand side of Eq. (8):

$$\Delta S_s = \frac{\Delta\sigma_s}{t^{\frac{2-m}{2m}} \cdot I(r)^{\frac{1}{m}}} \qquad (9)$$

where the thickness term $t^{(2-m)/2m}$ becomes unity for t =1 (unit thickness) and therefore, the thickness t can be interpreted as a ratio of actual thickness t to a unit thickness, rendering the term dimensionless. With this interpretation, the equivalent ΔS_s retains a stress unit. It is worth noting that the equivalent structural stress parameter described by Eq. (9) captures the stress concentration effects ($\Delta\sigma_s$), thickness effects (t), and loading mode effects (r) on fatigue behaviour.

3.4 Initial Crack Size Effects

Before Eq. (9) can be used to construct a single master S-N curve for welded joints, assumptions in performing the integration and the effects of M_{kn} on $I(r)$ must be quantified. It is well known that initial crack size (a_i / t) can make a significant difference in the final life prediction based on fracture mechanics as described in Eqs. (6-8).

The effects of a series of assumed initial crack sizes are shown in Fig. 9 by using the edge crack based K solution. Note that $I(r)$ is presented as $I(r)^{1/m}$ after considering the exponent 1/m in Eq. (11) to facilitate the comparison between Figs. 11a and 11b. Without considering the local notch effects, i.e., M_{kn}, different initial crack sizes a_i / t produce significantly different $I(r)^{1/m}$ curves as a function of r. Once M_{kn} is considered, the dependency of $I(r)$ on initial crack size a_i / t becomes insignificant, particularly for the two cases with small initial crack size (a_i / t), as shown in Fig.11b. The increase in $I(r)^{1/m}$ is about 8.5% as r increases from r = 0 (pure membrane) to r = 1 (pure bending) under load controlled conditions. This implies that with a strong notch effects in typical welded joints characterized by M_{kn}, the initial crack size effects on life predictions observed in typical fracture mechanics specimens without stress risers are significantly diminished in welded joints. Based on Fig. 9b, a_i / t=0.001 will be used in the rest of this paper.

3.5 S-N Data Correlation

The ultimate test for proving if the equivalent stress parameter (Eq. 9) is valid is to demonstrate that a large amount of experimental S-N data can be collapsed into a single narrow band. To do so, a large amount of S-N data (over 800 fatigue tests) from drastically different joint geometries, plate thicknesses and loading modes were collected from literature (see Fig. 10).

For each set of specimens and fatigue tests the structural stress calculations were performed under given loading conditions and failure criteria. The results are summarized in Fig. 11 in terms of both nominal stress range, and the equivalent structural stress range as given in Eq. (9). A wide scatter that results from using nominal stress can be seen in Fig. 11a, which is expected. Once the equivalent structural stress range is used according to Eq. (9), all the S-N data are collapsed into a narrower band, regardless of the diverse joint types, plate thicknesses, and loading modes under which the fatigue tests were conducted. The same methodology has been proven with the same effectiveness in correlating tubular and pipe/vessel joints [8].

By regression analysis, the mean line of Fig. 11b can be represented in the form of:

$$\frac{\Delta\sigma_s}{t^{\frac{2-m}{2m}} I(r)^{\frac{1}{m}}} = CN^{-\frac{1}{m'}} = 16308 \times N^{\frac{-1}{3.333}} \qquad (10)$$

with the stress unit in MPa and thickness in mm. and m = 3.6. In Eq. (10), $1/m'$ represents the negative slope of the master S-N curve in Fig. 11b. Note that in various publications $m = m'$ (=3 for steel welds) is often assumed. In this investigation, it is found that they are close but not necessarily the same. For simple fatigue test specimens nominal stresses are often well-
defined, then,

$$\Delta\sigma_s = SCF_{ss} \times \Delta S_n$$

in which SCF_{ss} signifies the structural stress based SCF and ΔS_n the typical nominal stress range definition.

For a given simple joint specimen of interest, the structural stress based SCF can be calculated using the present structural stress procedure. Then, the nominal stress based S-N behavior can be predicted by using the master S-N curve from Eq. (10) as:

$$\Delta S_n = C\left(\frac{t^{\frac{2-m}{2m}} I(r)^{\frac{1}{m}}}{SCF_{ss}}\right) N^{-\frac{1}{m'}} \qquad (11)$$

Both C and m' are given in Eq. (10) based on the master S-N database generated in this investigation. Two examples are given in Fig. 12. The mean nominal stress S-N curves for various plate thicknesses are predicted using Eq. (11) for the cruciform joint tests under remote tension loading by Maddox [13], and T-fillet joint tests under 3-point bending reported in [14]. Good correlation between the test data and those predicted by the master S-N curve (Eq. 10) is evident.

4 CONCLUSION

The mesh-insensitive structural stress parameter can not only be calculated consistently with the demonstrated mesh insensitivity, but also has been shown to be an effective fatigue parameter to correlate the fatigue behaviour of welded joints regardless of joint geometries, loading modes and plate thicknesses. Furthermore, the structural stress parameter can be directly related to the far-field stress in a fracture mechanics context. As a result, a rapid K estimation scheme has been demonstrated to be effective for analyzing arbitrary joints in plate structures, as well as other joint types such as tubular joints, pipe and vessel welds. With the aid of fracture mechanics principles a master S-N curve approach has been developed by introducing an equivalent structural stress parameter which captures three well-known factors that contribute to fatigue behaviour in welded joints: (a) the stress concentration due to joint geometry; (b) the loading mode; and (c) the plate thickness. A large amount of S-N data has been collected and correlated by using the equivalent structural stress parameter. The present master S-N curve approach can simplify fatigue evaluation procedures for large and complete structures and significantly reduce testing requirements, since the S-N data transferability in the form of the equivalent structural stress parameter has been established.

5 REFERENCES:

5.1 Book

1. Hobbacher, A., “Fatigue Design of Welded Joints and Components: Recommendations of IIW Joint Working Group XIII-XV”, Abington Publishing, Abington, Cambridge, 1996.

5.2 Journal Article

2. “Fatigue strength Analysis of Offshore Steel Structures,” DNV RP –C203, May 2000.

5.3 Journal Article

3. “Guide for the Fatigue Assessment of Offshore Structures,” ABS, April, 2003

5.4 Conference Proceedings

4. Fricke W., “Recommended Hot-Spot Analysis Procedure for Structural Details of FPSO’s and Ships Based on Round-Robin FE Analysis”, ISOPE Proceedings, Stavanger, Noway, June 2001.

5.5 Conference Proceedings

5. Dong, P. and Hong, J.K., “Analysis of Hot Spot Stress and Alternative Structural Stress Methods,” Proceedings of 22nd International Conference on Offshore Mechanics and Arctic Engineering, June 8-13, 2003, Cancun, Mexico.

5.6 Conference Proceedings

6. Healy, B.E., “A Case Study Comparison of Surface Extrapolation and Battelle Structural Stress Methodologies,” Proceedings of the 23rd International conference on Offshore Mechanics and Arctic Engineering, June 20-25, 2004, Vancouver, British Columbia, Canada.

5.7 Journal Article

7. Dong, P., *International Journal of Fatigue*, 23, pp. 865-876, 2001

5.8 Journal Article

8. Dong, P., Hong, J.K., Osage, D., and Prager, M., “Master S-N curve approach for welded components,” Welding Research Council Bulletin, No. 474, December, 2002, New York, New York, 10016.

5.9 Conference Proceedings

9. Dong, P., “A Robust Structural Stress Method for Fatigue Analysis of Ship Structures,” Proceedings of the 22nd International Conference on Offshore Mechanics and Arctic Engineering, June 8-13, 2003, Cancun, Mexico.

5.10 Journal Article

10. Zerbst, U., Heerens, J., and Schwalbe, K.-H., *Engineering Fracture Mechanics*, 69, 2002, pp. 1093-1100.

5.11 Journal Article

11. Tanaka, K., and Nakai, Y., Fatigue of Engineering Materials and Structures, Vol. 6, No.4, pp.315-327, 1983

5.12 Journal Article

12. Shin, C.S., and Smith, R.A., Engineering Facture Mechanics, Vol. 29, No.3, pp.301-315, 1988

5.13 Journal Article

13. Dong, P., Hong, J.K., and Cao, Z., *Int. J. of Fatigue*, Vol. 25(9-11), pp. 811-825, 2003.

5.14 Book

14. Maddox, S.J., *The Effect of Plate Thickness on the Fatigue Strength of Fillet Welded Joints*, The Welding Institute, Abington Hall, Abington, Cambridge CB1 6AL, 1987.

5.15 Journal Article

15. SR202 of Shipbuilding Research Association of Japan, *Fatigue Design and Quality Control for Offshore Structures*, 1991 (in Japanese).

6 FIGURES

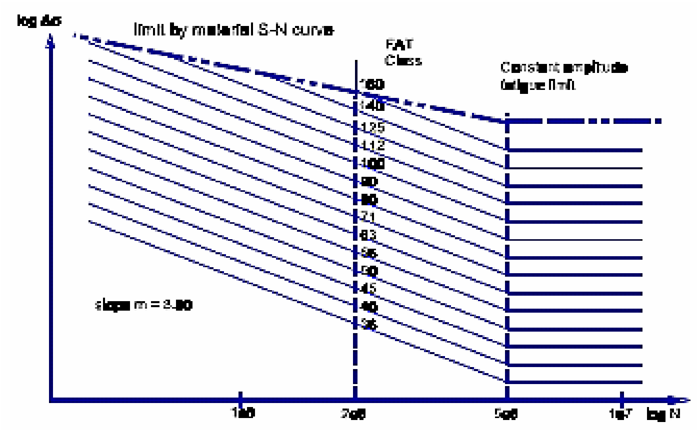

Figure 1. Fatigue S-N (or FAT) curves recommended by the IIW, based on nominal stress [1].

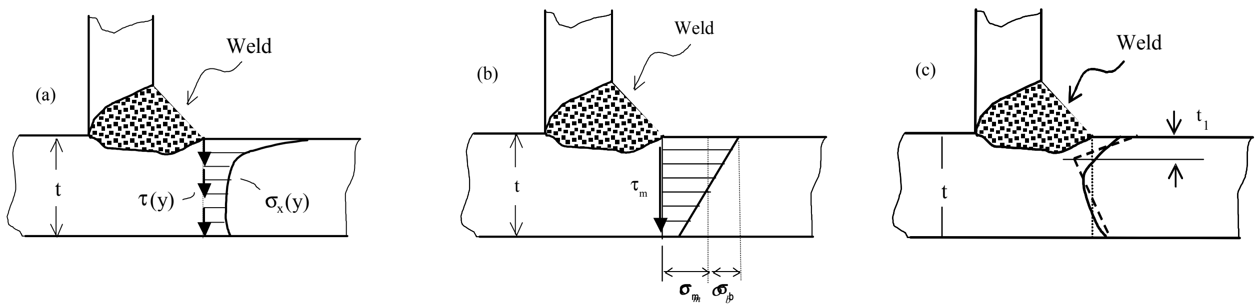

Figure: 2 Through-thickness structural stress definition: (a) local stresses from FEA model nodal forces; (b) structural stress or far-field stress; (c) self-equilibrating stress – solid line – and structural stress based estimation with respect to t_1 – dashed line.

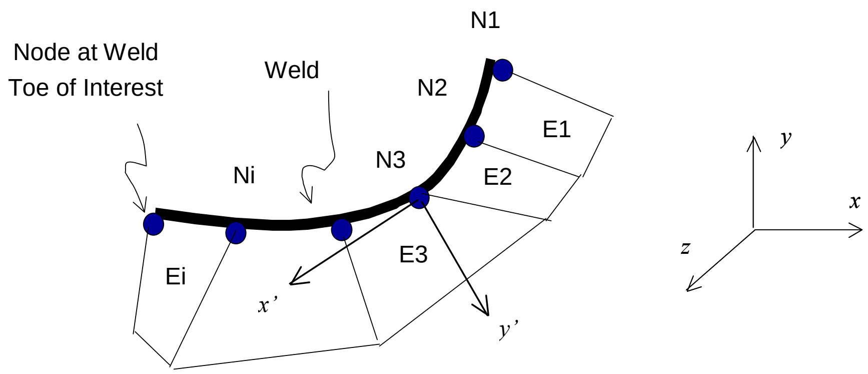

Figure 3: The structural stress calculation procedure for an arbitrarily curved weld using shell/plate elements.

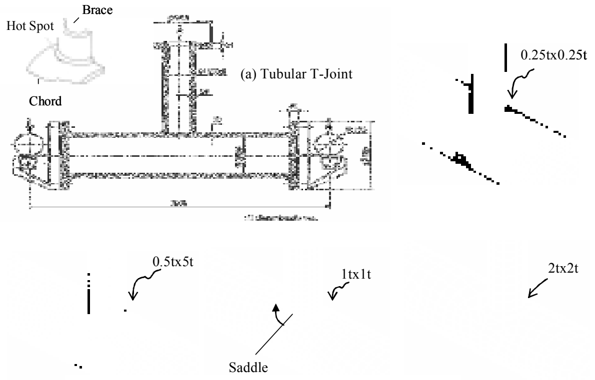

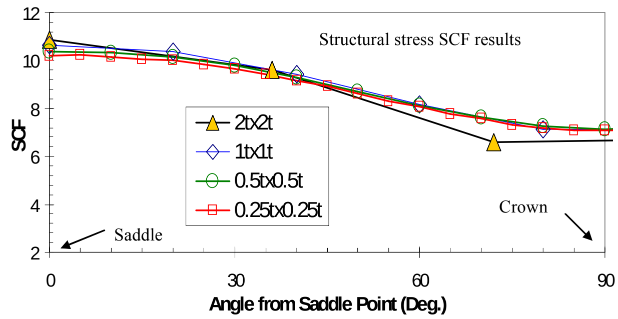

(a) Tubular joint with four mesh sizes

(b) Calculated structural stress for the four mesh sizes

Figure 4: Structural stress calculations for a tubular T-joint investigated by Zerbal et. al. [10], with four different mesh sizes. Comparison of the structural stresses along the weld toe at the chord.

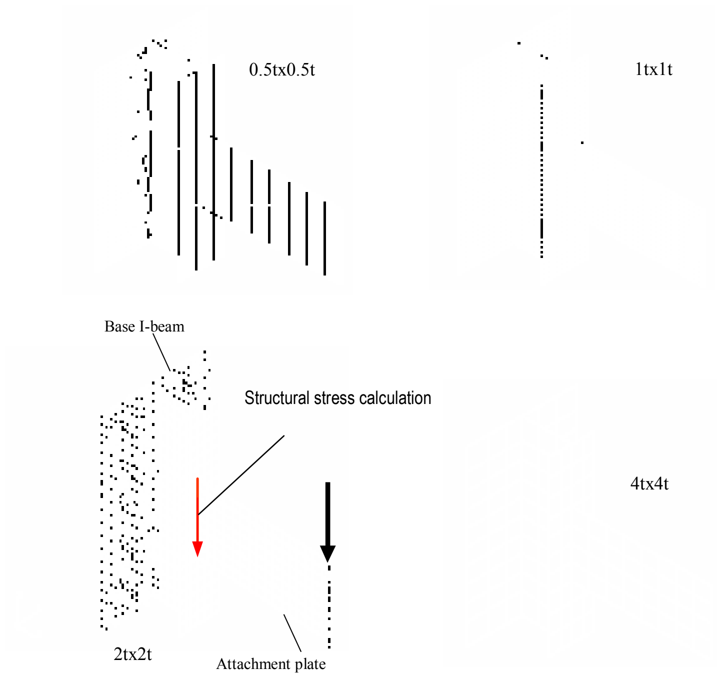

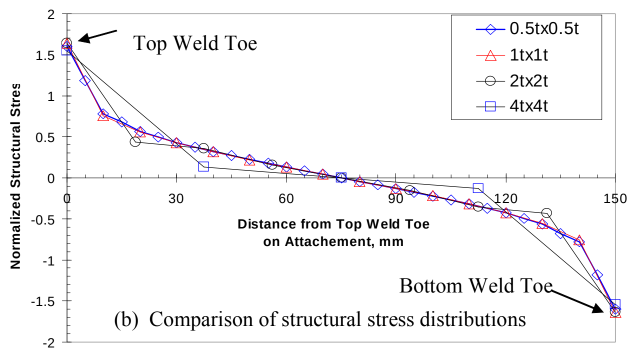

(a) FE models with four different mesh sizes.

(b) Comparison of structural stress distributions

Figure: 5. Mesh-size insensitivity for a plate to I-beam joint used in [1]. (a) FE models with very different mesh sizes; (b) comparison of structural stress along the weld toe on the attachment plate.

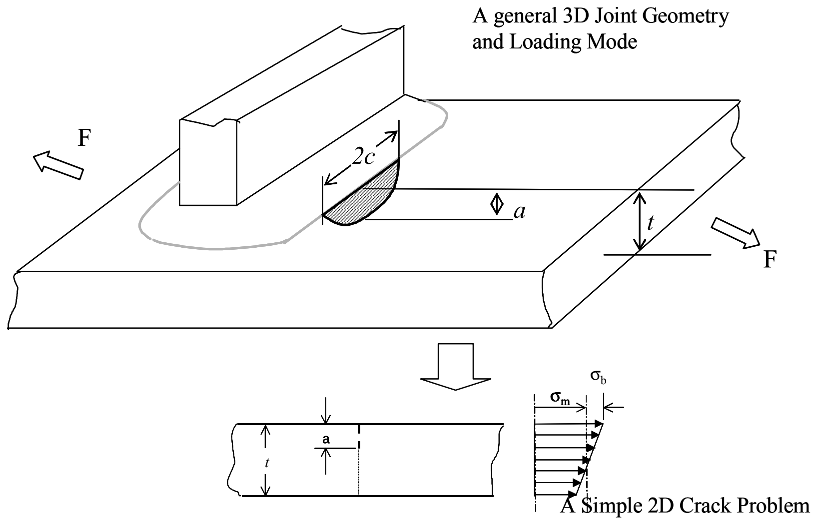

Figure: 6. Structural stress based transformation and K calculation using a simple fracture mechanics specimen

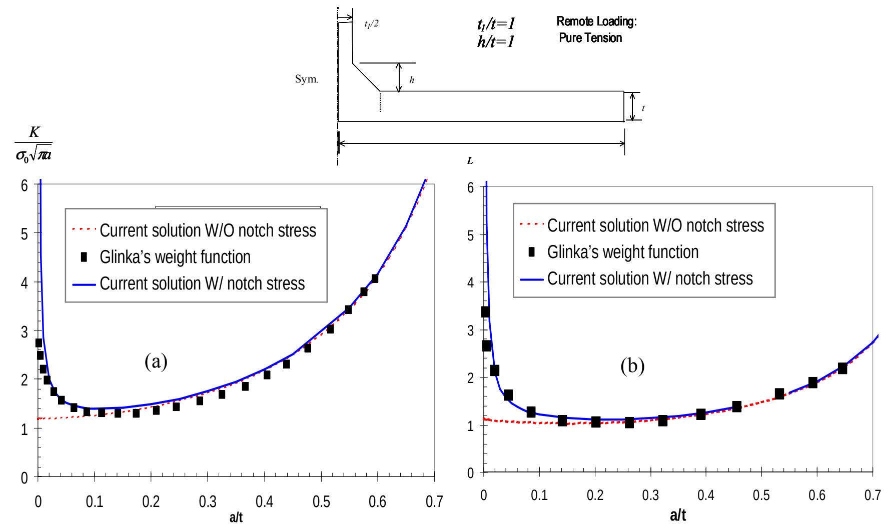

Figure: 7. Validations of the structural stress K estimation for a T-fillet joint using Glinka's weight function method [8]. (a) Remote bending. (b) Remote tension.

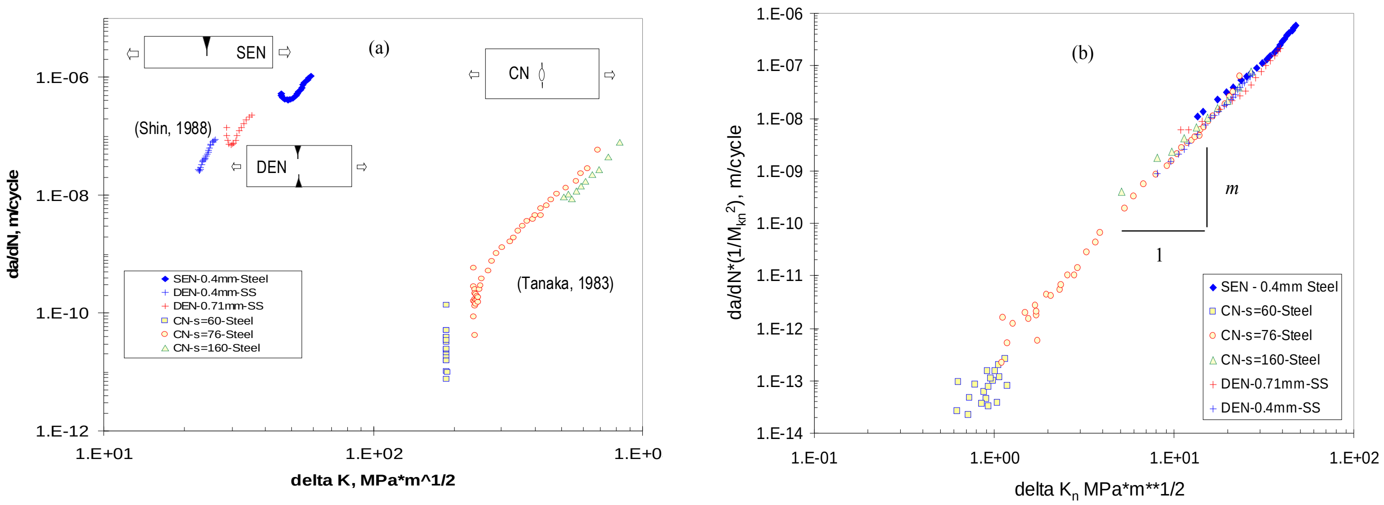

Figure: 8. Consolidation of short crack growth data from various specimen types and notch geometries [11,12] using the current two stage growth model with n=2. (a) *da/dN* versus nominal ΔK range – referred to as anomalous crack growth in [11, 12]. (b) current two-stage crack growth model

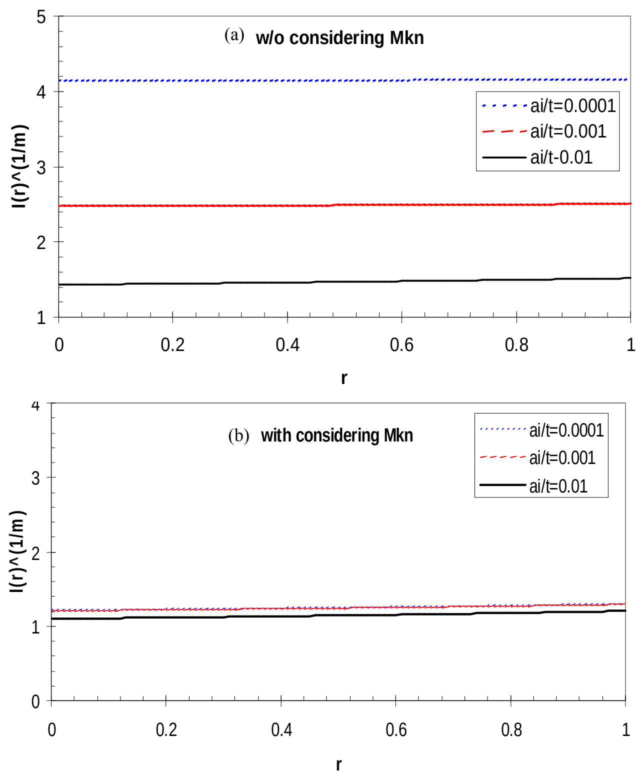

Figure: 9. Comparisons of *I(r)* functions with and without M_{kn}, and effects of initial *a/t*, for the edge crack solution. (a) without considering M_{kn}. (b) with consideration of M_{kn}.

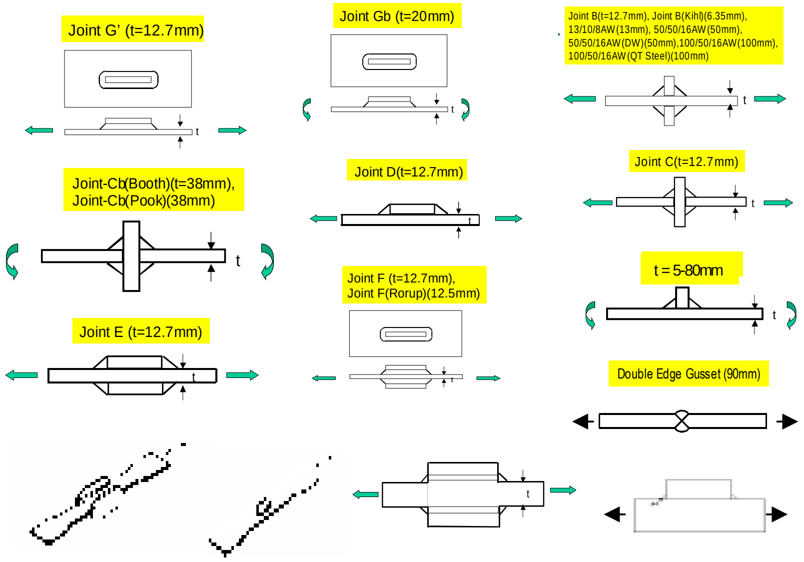

Figure:10. Illustration of some of the representative joint types analyzed in this investigation to develop the master S-N curve.

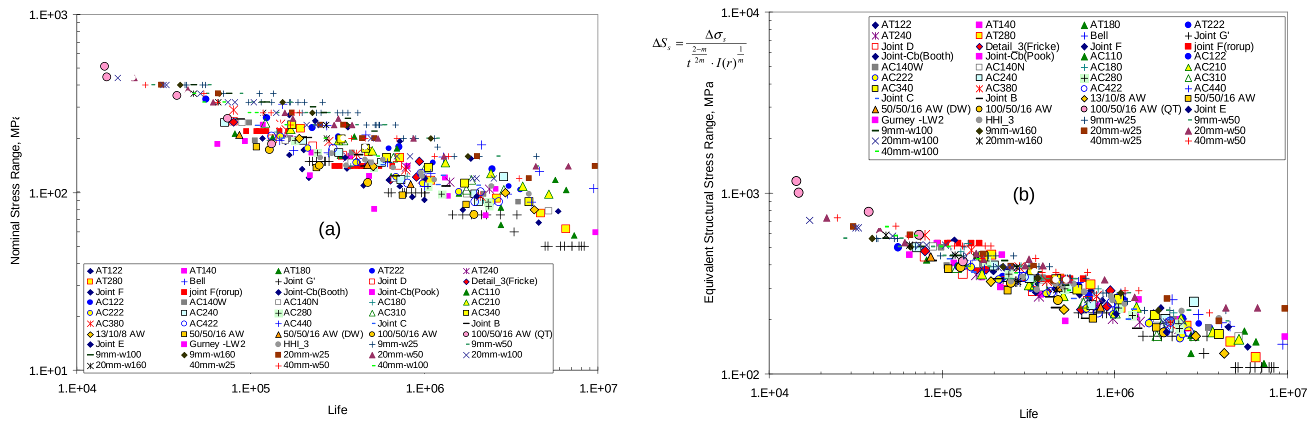

Figure: 11. Correlation of existing S-N data for various joint types, loading modes and plate thicknesses. (a) Nominal stress range versus life. (b) Equivalent structural stress range versus life.

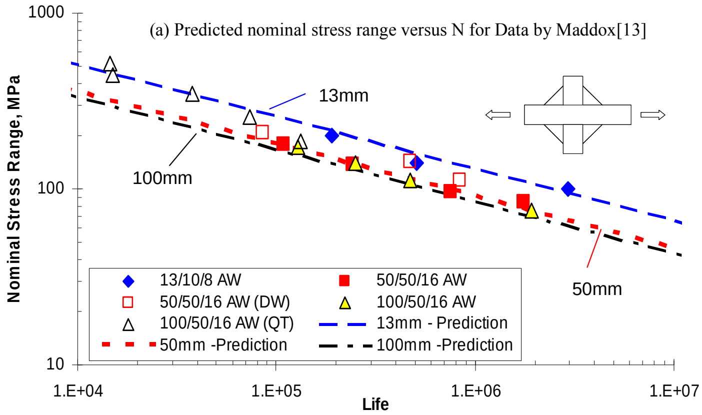

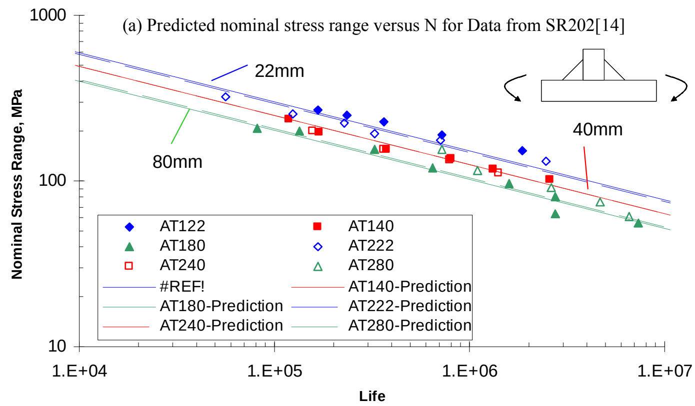

Figure: 12. The use of the master S-N curve (mean line) for the prediction of nominal stress range versus life curves generated by Maddox [13] and SR202 [14].